

Local periodic forcing of CO oxidation on a Pt(110) surface

This article has been downloaded from IOPscience. Please scroll down to see the full text article.

2003 New J. Phys. 5 60

(<http://iopscience.iop.org/1367-2630/5/1/360>)

View [the table of contents for this issue](#), or go to the [journal homepage](#) for more

Download details:

IP Address: 141.14.132.170

The article was downloaded on 23/03/2012 at 10:50

Please note that [terms and conditions apply](#).

Local periodic forcing of CO oxidation on a Pt(110) surface

J Wolff and H H Rotermund

Fritz-Haber-Institut der Max-Planck-Gesellschaft, Faradayweg 4-6,
Berlin D 14195, Germany

E-mail: rotermun@fhi-berlin.mpg.de

New Journal of Physics 5 (2003) 60.1–60.12 (<http://www.njp.org/>)

Received 7 February 2003

Published 6 June 2003

Abstract. The effect of local periodic forcing on uniformly oscillating CO oxidation on a Pt(110) surface is investigated utilizing our recently developed addressable catalyst approach. The heating, provided by a focused laser beam, serves as the locally applied external force. The observations are ascribed to the interaction between local actuation and global coupling through the gas phase leading to the suppression of the locally developed patterns.

Contents

| | |
|--|-----------|
| 1. Introduction | 1 |
| 2. Experiment | 2 |
| 3. Results | 3 |
| 3.1. $\omega_{ext}/\omega_0 < 1$ | 3 |
| 3.2. $\omega_{ext}/\omega_0 \gg 1$ | 6 |
| 3.3. $\omega_{ext}/\omega_0 \approx 1$ | 7 |
| 4. Summary | 11 |
| Acknowledgments | 11 |
| References | 11 |

1. Introduction

Periodic perturbations or a periodic forcing of oscillations are widespread phenomena in nature. One example is the changing of the seasons due to periodic variations of the inclination of the Earth on her orbit around the Sun. Oscillating ocean tides caused by the gravitational forces between the Moon, Earth and Sun is another example. These periodically forced systems are of

global dimensions and are, of course, not really controllable. An additional familiar example is the human heart: without other external stimuli the sinus node causes the heart to beat with a frequency of about $70 \text{ beats min}^{-1}$. Usually taken for granted, the heart's comforting periodic beating might suddenly change rhythm and establish a disastrous chaotic state, often resulting in an untimely death. A decade ago Winfree [1] described this kind of turbulence within the heart muscle as scroll waves in an excitable medium with a tendency of breaking up. Recent theoretical studies have shown that weak uniform forcing might suppress scroll waves in excitable media and that such a devastating course of events might thereby be avoidable [2].

The theory of forcing a single nonlinear oscillator is well established, exhibiting among other features quasi-periodicity and entrainment (e.g. [3, 4]). Recent work has focused on global forcing of distributed systems to determine if similar phenomena can also be found in these systems [5]. In addition, distributed systems show special types of patterns when they are globally forced [6]–[11]. Examples include labyrinthine standing wave patterns, bubble-shaped patterns and clusters.

CO oxidation on a Pt(110) surface (the model system discussed here) has been studied extensively. Initially, research on global forcing explored the response of the system without spatially resolving the concentration patterns [12]–[14]. Current investigations have focused on the spatio-temporal patterns generated by global forcing [15].

In contrast, this paper investigates the effects of *local* periodic forcing of CO oxidation on Pt(110). An example of local (although non-periodic) forcing within our solar system is the sweeping path of the Moon's shadow across the Earth during a total solar eclipse: the sudden darkness results in a sharp drop of temperature and an abrupt pause of all activity. In our experiment we do just the opposite by illuminating a circle repetitively on our catalytic surface with a focused laser beam, thereby creating a slight temperature increase along the path of the laser spot. In this investigation we restrict ourselves to local periodic forcing of the homogeneously oscillating CO oxidation on Pt(110).

2. Experiment

The experimental set-up is schematically shown in figure 1. The 10 mm diameter Pt(110) single crystal sample is kept in an UHV chamber, which is equipped with a low-energy electron diffraction (LEED) system, Ar-ion sputtering and sample heating (from the rear side) via a halogen lamp. The sample was prepared by repeated cycles of Ar^+ sputtering and O_2 treatment at 570 K, and subsequent annealing up to 1000 K. Gas supplies for CO and O_2 were automated and stabilized, allowing for controlled settings of the partial pressures of the reactants within the UHV chamber. Adsorbate concentration patterns on the surface of the sample were imaged using ellipsomicroscopy for surface imaging (EMSI) [16], shown schematically by the green beam path originating from the first Ar-ion laser presented in figure 1.

In this work, we have chosen the settings of the optical elements (polarizer, compensator and analyser) such that the CO-covered states of the sample are imaged as white areas, while the dark regions represent oxygen-covered areas. The resulting sequences of images are used to calculate locally resolved frequency spectra by using the local evolution of the concentrations represented by grey values in the images as time series.

To apply local periodic forcing we use a second Ar-ion laser (the blue beam path presented in figure 1) which is focused to a spot of about $50 \mu\text{m}$ diameter. The focused laser gives rise to a local temperature increase which changes the dynamics of the reaction diffusion system—

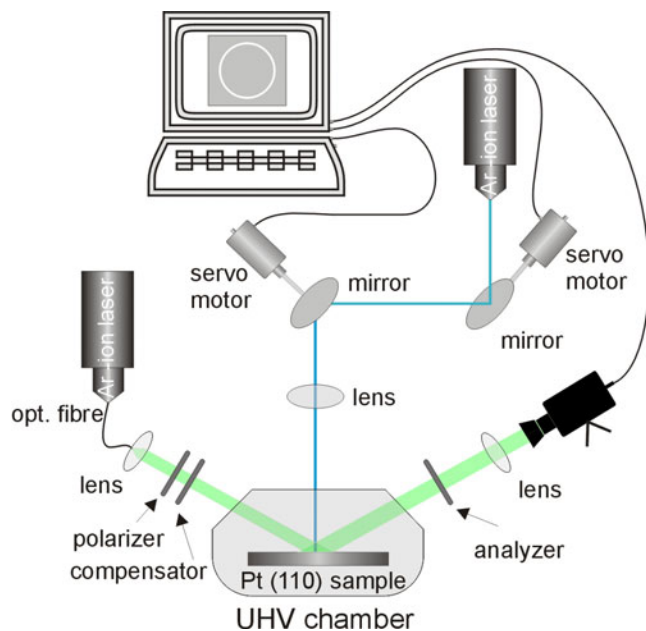


Figure 1. Sketch of the experimental set-up. The green beam path shows the EMSI, while the blue beam path shows the set-up for the heating laser. The laser beam positioning mirrors are mounted perpendicular to each other, and are controlled by computer utilizing servomotors.

mainly by desorbing CO [17]–[19]. Two computer-controllable mirrors move the laser spot with constant angular velocity along a circular path on the sample, thus heating each point along this path periodically. A laser power of 3 W corresponding to a maximum temperature increase of about 20 K is used. Compared to the dynamics of the reaction, which is in the order of seconds, any change of the local temperature due to the laser heating happens very quickly: it takes less than 5 ms to obtain 63% of the total temperature increase reached after 1 s of irradiation.

All experiments were performed in a state where the unperturbed reaction shows homogeneous oscillations at a temperature of about 535 K. The partial pressures for the reactants were kept at $p_{\text{CO}} = 9 \times 10^{-5}$ mbar and $p_{\text{O}_2} = 3.0 \times 10^{-4}$ mbar.

3. Results

The observed phenomena can be divided into three categories according to the relation between the frequency of the external perturbation ω_{ext} and the frequency of the unperturbed inherent oscillation of the reaction ω_0 : $\omega_{\text{ext}}/\omega_0 < 1$, $\omega_{\text{ext}}/\omega_0 \approx 1$ and $\omega_{\text{ext}}/\omega_0 \gg 1$. Examples of observations for all three regions are shown in figure 2. Short versions of the corresponding original movies are available as links within the appropriate figure captions.

3.1. $\omega_{\text{ext}}/\omega_0 < 1$

If ω_{ext} is considerably smaller than ω_0 , the temperature heterogeneity created by the laser spot needs more than one period (T_0) of the oscillation for one revolution around the circle. In the case where exactly three periods occur during one complete circle, three, apparently stationary,

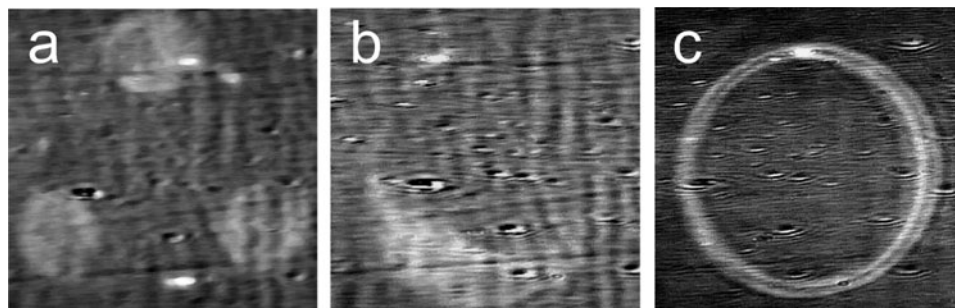


Figure 2. (a) The period for one revolution of the laser spot is about $3T_0$. The image was put together from three images of consecutive dark phases of the global oscillation and shows three bright regions, which appear one after the other (taken with permission from [18]) (movie2a). (b) Snapshot for $\omega_{ext}/\omega_0 \approx 1$ (movie2b). (c) Snapshot for $\omega_{ext}/\omega_0 = 8.78$ (movie2c). For all measurements the diameter of the circle is $880 \mu\text{m}$. Other parameters: laser power $L_p = 3 \text{ W}$, $p_{\text{O}_2} = 3.0 \times 10^{-4} \text{ mbar}$, $T = 538 \text{ K}$ (a, b), $T = 535 \text{ K}$ (c), $p_{\text{CO}} = 9.2 \times 10^{-5} \text{ mbar}$ (a, b), $p_{\text{CO}} = 8.9 \times 10^{-5} \text{ mbar}$ (c).

white spots (the CO-covered state of the sample) are observed consecutively during the dark (oxygen covered) phase of the oscillation—one per oscillation (figure 2(a)). For these apparently stationary spots the ratio of the period of one revolution of the temperature heterogeneity around the circle (T_{ext}) and T_0 is either an integer or a rational number with a small denominator. (For example, three apparently stationary spots are also observable for $T_{ext}/T_0 = 3/2$, they just appear in a different order.)

When the period of one temperature heterogeneity revolution (T_{ext}) is not a (small digit) rational multiple of T_0 , the white spots are still present. However, in contrast to the example shown in figure 2(a), they are no longer stationary but seem to move along the circle. An example for this is given in figure 3, which shows two space–time plots that were produced parallel to the path of the laser spot outside the circle at a distance of $75 \mu\text{m}$. Figure 3(a) displays the space–time diagram that belongs to figure 2(a). The perturbations, caused by the laser, appear roughly at the same positions along the circle as demonstrated by the white dashed line that runs nearly horizontal. Only a small drift is visible, which means that ω_{ext} is quite close to $1/3\omega_0$. Figure 3(b) belongs to a measurement where $\omega_{ext} = 0.36\omega_0$. In this example the perturbations are moving around the circle much faster, again indicated by a white dashed line, that has a considerably larger slope compared to the one given in figure 3(a). However, any single perturbation still needs about 37 oscillations to make one full revolution. This corresponds to a frequency mismatch of $1/37 \approx 0.\overline{027}$, which fits nicely with the measured relation between ω_{ext} and ω_0 ($0.\overline{3} + 0.\overline{027} = 0.360$).

The small inset presented in figure 3(a) magnifies one perturbation of the space–time plot. It gives the first hint regarding the mechanism that is responsible for the appearance of the white regions during the dark phases of the oscillations. For further illumination a space–time plot is taken along a linear cut through the circular path of the temperature heterogeneity. Only one side of this profile, with the laser path indicated by an arrow on the left-hand side, is presented in figure 4.

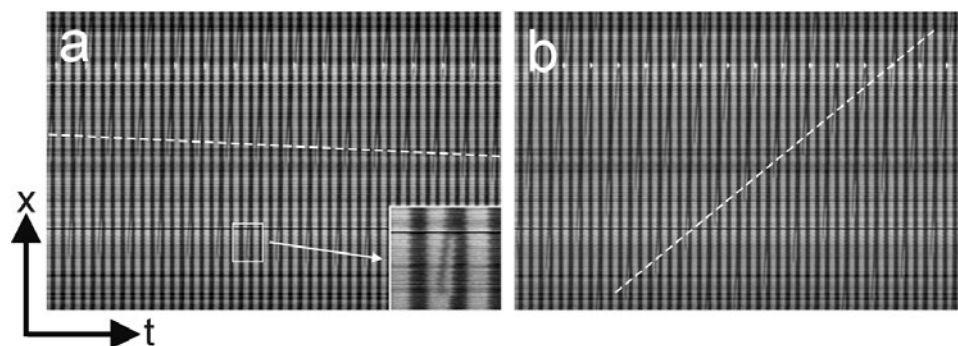


Figure 3. (a) Space–time plot ($3240 \mu\text{m} \times 32 \text{ s}$) taken parallel to the laser’s path (a distance $75 \mu\text{m}$ outside the circle) for the same measurement as presented in figure 2(a). The white dashed line shows that the white spots are moving only slightly along the circle. The inset is a magnified area as indicated by the arrow (taken with permission from [18]). (b) Space–time plot for $\omega_{ext} = 0.36\omega_0$. The perturbation moves considerably faster around the circle—again indicated by a white dashed line (movie3b).

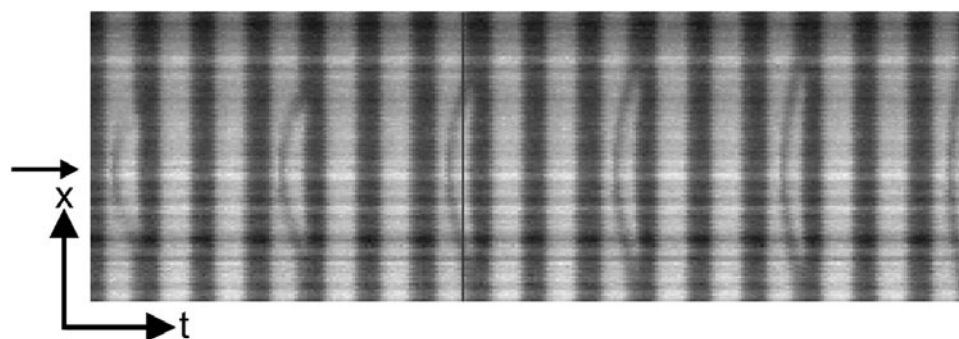


Figure 4. Space–time plot ($380 \mu\text{m} \times 11.1 \text{ s}$) for the measurement displayed in figure 2(a) taken along a cut through the laser’s path (indicated by the small black arrow). The start of the dark phase of the homogeneous oscillation is marked in one place by a thin vertical line in order to show the phase delay caused by the emitted wave.

There, during the first part of the CO-covered phase, an oxygen wave is emitted from the position of the laser spot’s path. As time progresses, this oxygen wave causes the slightly delayed appearance of the regular oxygen-covered phase from the intrinsic oscillation. The area affected spreads with time, since the oxygen wave propagates slowly. The waves are not emitted during every CO-covered phase of the oscillation but only when the temperature heterogeneity passes this particular part of the circle. Therefore, only after every third oscillation is a wave created, due to the fact that we had chosen ω_{ext} to be approximately $1/3\omega_0$.

Returning to figure 3, we see that the perturbation is created only during the CO-covered bright phase of the oscillation. During the oxygen-covered phase of the oscillation the local heating does not seem to have any effect. This is also observable in the space–time plot cutting through the opposite side of the circle (not included in figure 4). There is no emission of oxygen waves, while the laser visits this point only during the dark phase of the oscillation. This is true

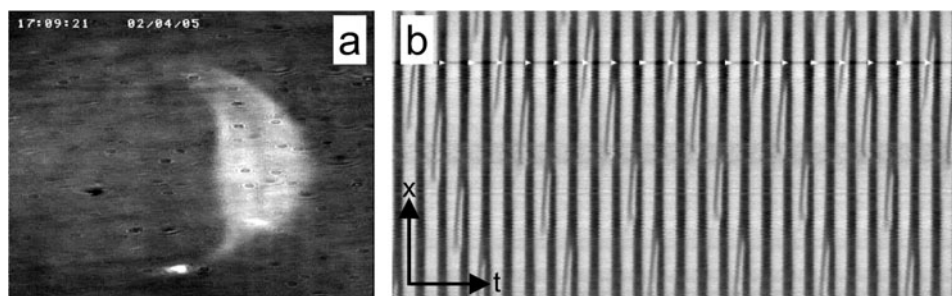


Figure 5. (a) Snapshot of a perturbation during the dark phase of the oscillation (movie5). Space-time plot taken parallel to the laser's path (at a distance of $75 \mu\text{m}$ outside of the circle, for about 18.5 s). Parameters: $\omega_{ext} = 0.72\omega_0$, $p_{\text{CO}} = 9.2 \times 10^{-5} \text{ mbar}$, $p_{\text{O}_2} = 3.0 \times 10^{-4} \text{ mbar}$, $T = 538 \text{ K}$.

only for odd ratios between ω_0 and ω_{ext} . Of course, for even ratios both points of intersection will emit oxygen waves during CO-covered phases. Therefore, it can be deduced that the main effect of the local increase in temperature is the increased desorption of CO, which is most likely to occur when the sample is CO covered.

This observation leads to a deduction that can be tested experimentally: if indeed the laser affects the pattern formation mainly during the CO-covered phase of the homogeneous oscillation, then the size of the resulting perturbation should depend on the length of the path travelled by the laser spot during the bright phase. The faster the laser spot travels the more CO-covered area it will influence, and the resulting perturbation should be proportionally greater. Indeed the size of the perturbation increases with increasing speed of the laser spot. An example for $\omega_{ext} = 0.72\omega_0$ is shown in figure 5. Both the snapshot of figure 5(a) and the corresponding space-time plot taken parallel to the laser's path (figure 5(b)) show a significantly increased perturbation.

3.2. $\omega_{ext}/\omega_0 \gg 1$

In this case, $\omega_{ext} \gg \omega_0$, the temperature heterogeneity performs multiple revolutions on its circular path during one oscillation of the reaction. An example for $\omega_{ext} = 8.78\omega_0$ is shown in figure 6. The time-series presented in figure 6(a) shows that the whole circle is affected nearly identically, as if the laser was heating the whole circle simultaneously. The space-time plot presented in figure 6(b) shows only a very weak perturbation at the cut through of the laser's path, which corresponds to the emission of a weak oxygen wave.

The fact that the emitted wave is weaker than in the preceding examples is due to the same effect. As the laser moves around the circle faster, it heats any point along the circle for a shorter time. Therefore, the temperature increase ΔT , which is responsible for the perturbation of the homogeneous oscillation, becomes smaller even though the total energy delivered to the sample stays the same for all experiments, a prerequisite to perform the experiments at constant sample temperatures.

Decreasing ω_{ext} , e.g. $\omega_{ext} = 4.76\omega_0$, leads to the intermediate state shown in figure 7. In the series of snapshots presented in figure 7(a) the circle does not appear as if it was being heated uniformly. The perturbation reveals a clear structure along the circle. Figure 7(b) shows a space-time plot of a cut through the laser's path. In this case, the temperature heterogeneity is

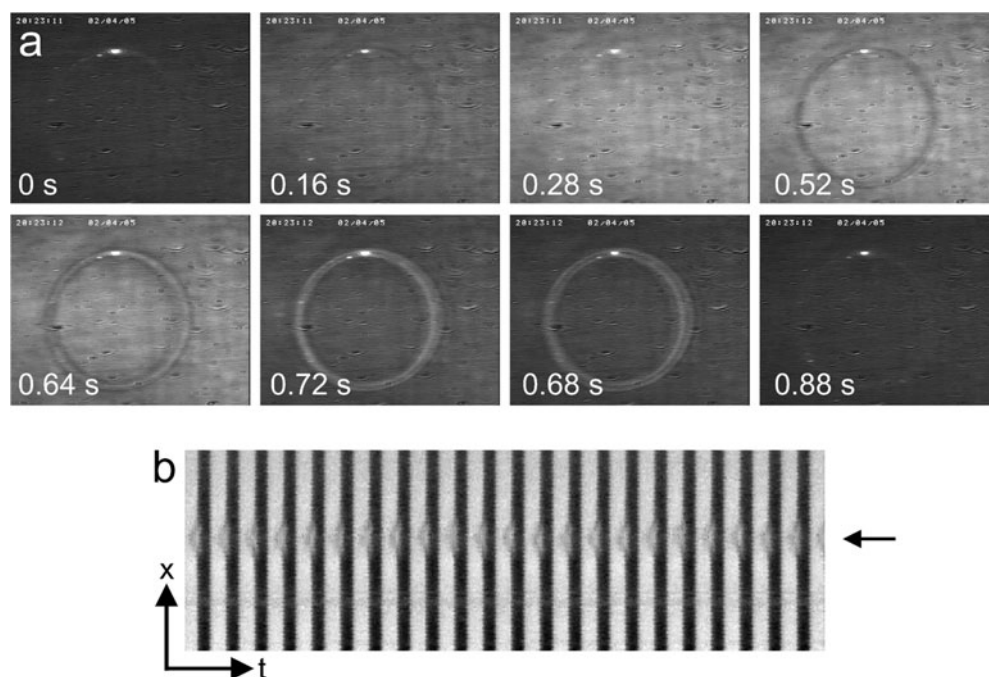


Figure 6. (a) Sequence covering one period of the global oscillations. (b) Space-time plot ($430 \mu\text{m} \times 21 \text{s}$) taken along a cut through the laser's path (marked by the black arrow). Parameters: $\omega_{ext} = 8.78\omega_0$, $T = 535 \text{ K}$, $p_{\text{CO}} = 8.9 \times 10^{-5} \text{ mbar}$, $p_{\text{O}_2} = 3.0 \times 10^{-4} \text{ mbar}$.

even able to sometimes cause the emission of more than one wave during a bright phase of the oscillation. The first of the two emitted waves, however, does not propagate very far.

3.3. $\omega_{ext}/\omega_0 \approx 1$

Reducing ω_{ext} even further, the region where $\omega_{ext}/\omega_0 \approx 1$ is approached. Although the probability to detect entrainment should be largest for this region, it was not actually observed. Analysing the data for their own frequency spectra always reveals both frequencies ω_{ext} and ω_0 , with one exception. As an example for the general situation, the case of $\omega_{ext} = 1.12\omega_0$ is presented in figure 8(a). Peaks at 1.30 and 1.46 Hz are clearly visible with comparable amplitudes. The exception is represented by a measurement where $\omega_{ext} = 0.99\omega_0$ (figure 8(b)). In this case one can expect entrainment to occur if one could be sure that the frequency of the homogeneous oscillations had adapted to the forcing frequency. A strong argument for such harmonic entrainment would be the resonant enhancement for the amplitude.

However, as ω_0 was drifting slightly during the whole experiment it is not possible to conclude whether entrainment occurred or if, alternatively, only the resolution of the frequency spectrum was insufficient to resolve the two frequencies. A hint is given when looking at the distribution of ω_0 in space: as ω_0 is the same close to the laser's path as at some distance away from it, and since the space-time plot (figure 9) does not suggest that the forcing has any influence on the oscillations at that distance, it has to be concluded that indeed even for nearly identical frequencies ω_{ext} and ω_0 no entrainment occurs.

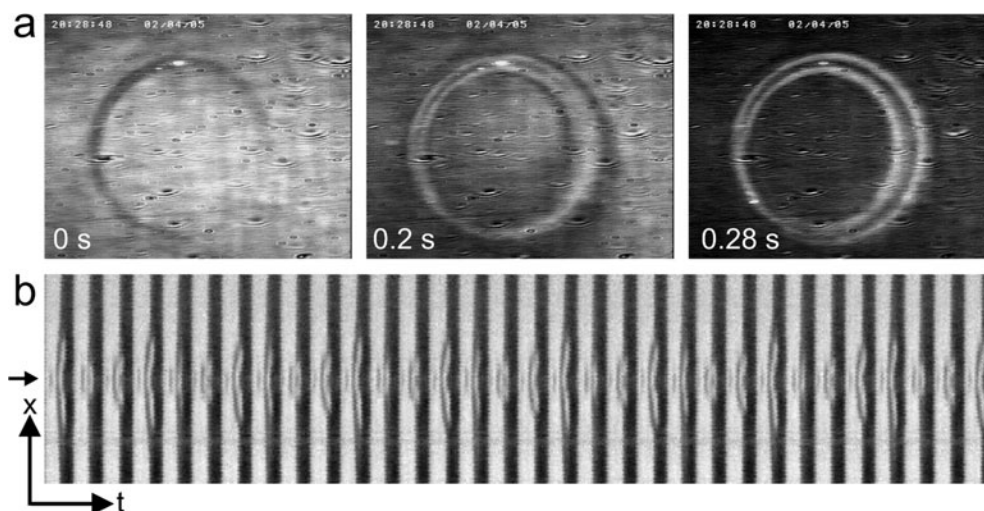


Figure 7. (a) Three snapshots showing that although the complete circle is affected by the laser spot, the perturbation shows a spatial structure because the laser is travelling slower than in figure 6 (movie7). (b) Space–time plot ($410 \mu\text{m} \times 32 \text{ s}$) along a cut through the laser’s path (indicated by black arrow) showing the repeated emission of oxygen waves. Parameters: $\omega_{ext} = 4.76\omega_0$, $T = 535 \text{ K}$, $p_{\text{CO}} = 8.9 \times 10^{-5} \text{ mbar}$, $p_{\text{O}_2} = 3.0 \times 10^{-4} \text{ mbar}$.

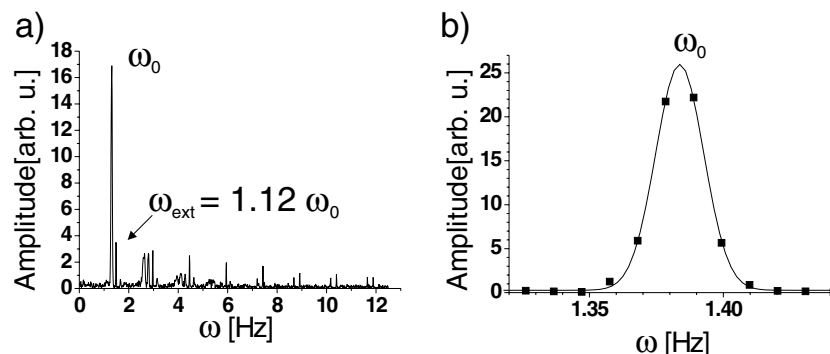


Figure 8. Two spectra measured directly on the laser’s path. (a) $\omega_{ext} = 1.12\omega_0$, (b) $\omega_{ext} = 0.99\omega_0$. In (a) both frequencies ω_{ext} and ω_0 are detected, while (b) only shows the region close to $\omega_{ext} = \omega_0$. The resolution of the spectrum is not sufficient to differentiate between ω_{ext} and ω_0 .

This observation leads to the following question: why was there no entrainment found, even under the most favourable conditions? One possible explanation would be that the applied strength of the forcing was too small. The regions where entrainment is usually found have a certain width as far as ω_{ext} is concerned depending on the amplitude of the forcing. But from looking at the sequences of snapshots, at the movies, and at the space–time plots this interpretation can be refuted, because the laser clearly has some impact on the pattern formation of the reaction. Analysing the shown space–time plots more closely (best seen in figure 4) it becomes apparent that the emitted oxygen wave is being suppressed by the appearance of the dark phase of the global oscillation. This part of the oscillation effectively resets the phase everywhere on the crystal thus

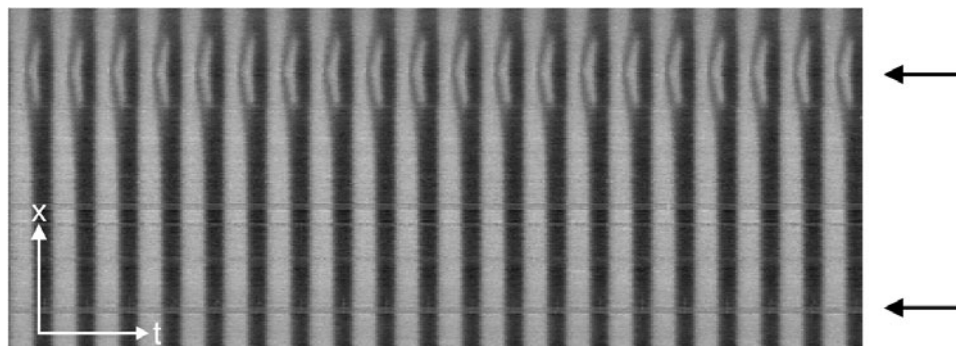


Figure 9. Space–time plot ($1.3 \text{ mm} \times 14.4 \text{ s}$) along a cut through the laser’s path (both points of intersection are marked by black arrows) for the measurement from figure 8(b). The homogeneous oscillation in a small distance from the circle seems to be unaffected by the perturbation. The second point, where the cut crosses the circle drawn by the laser, is included in the diagram (at the bottom) but does not show any wave emission. The laser spot creates only one perturbation, which is stationary on the other side of the circle. The part of the circle that is drawn during the dark phase of the oscillation (oxygen covered) is not visibly affected.

synchronizing the oscillation in space. This is not necessarily an expected behaviour of such a system. Usually, one would assume an emitted wave to propagate undisturbed as long as it does not meet another wave, which would then lead to annihilation [20, 21]. Here, another mechanism comes into play: as the whole surface is oscillating in phase, the consumption of CO through reaction is periodically modulated. This leads to global coupling through the gas phase [22]–[25] which stabilizes the homogeneous oscillation [26, 27] and suppresses the propagation of waves which would otherwise spatially desynchronize the oscillation on the crystal. Obviously, the global ‘forcing’ represented by the gas phase coupling supersedes any attempts of local forcing by the periodically increased temperature to alternate the oscillations. There are three possible approaches to limit the global coupling through the gas phase:

- (1) the catalytically active area could be reduced to the imaged field of view by using microlithography [28, 29]. Since in our experiments the typical imaged area is about $1.1 \times 1.1 \text{ mm}^2$, but the total single crystal surface has an area of about 80 mm^2 , a substantial reduction of the global coupling could be expected.
- (2) by increasing the volume of the reaction chamber a similar effect could be achieved as the relative impact of adsorption and desorption from the sample on the total partial pressure of the species would become smaller.
- (3) by increasing the pumping speed for the gases, the residual time for the reactants in the vessel would be shortened, thereby again limiting the strength of the gas phase coupling.

In the future, studies following the first approach are planned.

Although we have not found entrainment directly, we have tried to detect traces of it by analysing the obtained frequency spectra in more detail. Supposing that the two frequencies ω_{ext} and ω_0 do not interrelate, one would expect that the ratio of the two corresponding amplitudes $\phi = A_{ext}/A_0$ is independent of ω_{ext} . Considering additionally, that with increasing ω_{ext} the laser spot spends less time for each revolution of the circle, A_{ext} is steadily decreasing, therefore ϕ should be a monotonically falling function with ω_{ext} .

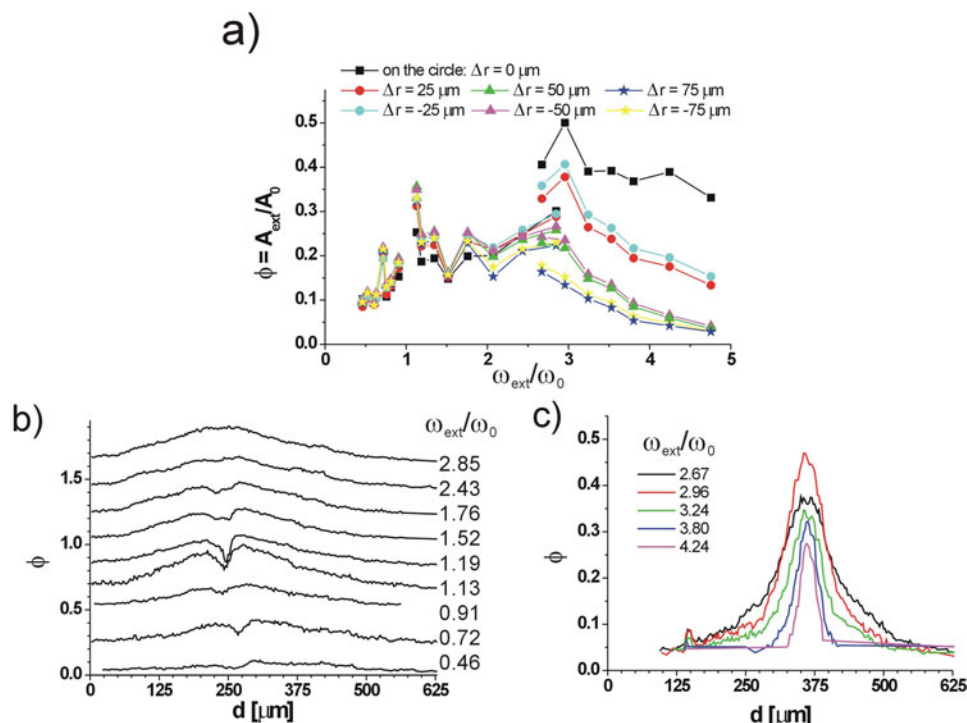


Figure 10. (a) Ratio $\phi = A_{ext}/A_0$ for different distances from the laser's path depending on ω_{ext}/ω_0 . (b) $\phi(x)$ for measurements close to $\omega_{ext}/\omega_0 = 1$. The curves have been shifted with respect to each other for better viewing. (c) $\phi(x)$ for measurements for $\omega_{ext}/\omega_0 > 1$.

We calculated ϕ as averages of all pixels on seven different circles—directly on the laser's path and on circles with radii both 25, 50 and 75 μm smaller and larger than the laser's path. The results of two different experiments overlapping between $2.5 < \omega_{ext}/\omega_0 < 3$ are displayed in figure 10(a) ($\omega_{ext} = 0.99\omega_0$ is not included, because ω_{ext} and ω_0 were not separately measurable).

Looking first at the data including the area around $\omega_{ext}/\omega_0 \approx 1$ a possible maximum around $\omega_{ext}/\omega_0 = 1$ catches the eye. Unfortunately only a single data point represents this maximum. Although coming from $\omega_{ext}/\omega_0 < 1$ there is—apart from one data point found for $\omega_{ext}/\omega_0 = 0.71$, which is well outside any expected region for entrainment (Arnol'd-tongue)—an increase in ϕ towards $\omega_{ext}/\omega_0 = 1$, the expected decrease for $\omega_{ext}/\omega_0 > 1$ is not observed. The ratio of amplitudes stays more or less constant with a rather large scattering. Therefore, it must be assumed that the data point suggesting the maximum is also due to scattering.

The second set of data, obtained for a slightly different set of reaction parameters and circle location, shows the expected decrease of ϕ with increasing ω_{ext}/ω_0 . Additionally, it displays a more pronounced dependence on the position for which ϕ was determined. ϕ is maximal exactly on the laser spot's path and decreases with increasing distance as would be expected for a local effect that is attenuated with distance.

Taking a closer look, the spatial dependence of ϕ is shown for several examples of ω_{ext}/ω_0 in figures 10(b) and (c). The graphs were obtained by calculating ϕ along a linear cut perpendicular to the laser spot's path. A single maximum of $\phi(x)$ is observable. The spatial extent of this maximum corresponds to the distance the emitted waves propagate before being swallowed by the global oscillation. Figure 10(c) shows that with increasing ω_{ext}/ω_0 , this range decreases.

Close to $\omega_{ext}/\omega_0 = 1$ an additional local minimum situated on top of the maximum is observed. It is much smaller for $\omega_{ext}/\omega_0 \neq 1$ and vanishes for $\omega_{ext}/\omega_0 > 2.4$.

4. Summary

Our experiments did not reveal any entrainment. The observed phenomena are explainable as a continuous transition from a slow moving temperature heterogeneity to a faster moving one. In all instances the laser heating creates oxygen waves during the CO-covered phase of the global oscillation by locally increasing the desorption of CO. These waves propagate a certain distance until they are suppressed by the oxygen-covered dark phase of the global oscillation, which is stabilized through coupling with the gas phase. The phase delay caused by the emitted waves leads to the observed bright regions just before synchronization. Determining the ratio of amplitudes $\phi(x)$ results in a measure for the effective spatial range of the local perturbation. In this case it corresponds to the distance the created waves propagate before being suppressed. Where the ratio between the external forcing frequency and the inherent oscillation frequency approaches unity, $\omega_{ext}/\omega_0 \approx 1$, we observe an unexplainable local reduction of $\phi(x)$.

Acknowledgments

We thank Yannis Kevrekidis for helpful discussions and Caryl Michaelson-Rotermund for suggestions to improve this paper.

References

- [1] Winfree A T 1994 Electrical turbulence in three-dimensional heart muscle *Science* **266** 1003
- [2] Alonso S, Sagues F and Mikhailov A S 2003 Taming Winfree turbulence of scroll waves in excitable media *Science* online January 30 2003; 10.1126/science.1080207
- [3] Schuster H G 1995 *Deterministic Chaos* (New York: VCH)
- [4] Thompson J M T and Stewart H B 1986 *Nonlinear Dynamics and Chaos* (Chichester: Wiley)
- [5] Couillet P and Emilsson K 1992 Strong resonances of spatially distributed oscillators: a laboratory to study patterns and defects *Physica D* **61** 119
- [6] Petrov V, Ouyang Q and Swinney H L 1997 Resonant pattern formation in a chemical system *Nature* **388** 655
- [7] Lin A L, Bertram M, Martinez K and Swinney H L 2000 Resonant phase patterns in a reaction–diffusion system *Phys. Rev. Lett.* **84** 4240
- [8] Lin A L, Hagberg A, Ardelea A, Bertram M, Swinney H L and Meron E 2000 Four-phase patterns in forced oscillatory systems *Phys. Rev. E* **62** 3790
- [9] Sendina-Nadal I, Mihaliuk E, Wang J C, Perez-Munuzuri V and Showalter K 2001 Wave propagation in subexcitable media with periodically modulated excitability *Phys. Rev. Lett.* **86** 1646
- [10] Vanag V K, Zhabotinsky A M and Epstein I R 2001 Oscillatory clusters in the periodically illuminated, spatially extended Belousov–Zhabotinsky reaction *Phys. Rev. Lett.* **86** 552
- [11] Martinez K, Lin A L, Kharrazian R, Sailer X and Swinney H L 2002 Resonance in periodically inhibited reaction–diffusion systems *Physica D* **168** 1
- [12] Eiswirth M and Ertl G 1988 Forced oscillations of a self-oscillating surface reaction *Phys. Rev. Lett.* **60** 1526
- [13] Eiswirth M and Ertl G 1988 Dynamic order in a surface process *Appl. Phys. A* **47** 91
- [14] Krischer K, Eiswirth M and Ertl G 1992 Periodic perturbations of the oscillatory CO oxidation on Pt(110): model calculations *J. Chem. Phys.* **97** 307

- [15] Bertram M, Beta C, Rotermund H H and Ertl G 2003 Complex patterns in a periodically forced surface reaction *J. Phys. Chem.* submitted
- [16] Rotermund H H, Haas G, Franz R U, Tromp R M and Ertl G 1995 Imaging pattern formation in surface reactions from ultra-high vacuum to atmospheric pressures *Science* **270** 608
- [17] Wolff J, Papathanasiou A G, Kevrekidis I G, Rotermund H H and Ertl G 2001 Spatio-temporal addressing of surface activity *Science* **294** 134
- [18] Wolff J, Papathanasiou A G, Rotermund H H, Ertl G, Katsoulakis M, Li X and Kevrekidis I G 2003 Wave initiation through spatiotemporally structured perturbations *Phys. Rev. Lett.* **90** 148301
- [19] Wolff J, Papathanasiou A G, Rotermund H H, Ertl G, Li X and Kevrekidis I G 2003 On the gentle dragging of reaction waves *Phys. Rev. Lett.* **90** 018302-1
- [20] Rotermund H H, Jakubith S, von Oertzen A and Ertl G 1991 Solitons in a surface reaction *Phys. Rev. Lett.* **66** 3083
- [21] Bär M, Eiswirth M, Rotermund H H and Ertl G 1992 Solitary-wave phenomena in an excitable surface reaction *Phys. Rev. Lett.* **69** 945
- [22] Jakubith S, Rotermund H H, Engel W, Oertzen a V and Ertl G 1990 Spatiotemporal concentration patterns in a surface reaction: propagating and standing waves, rotating spirals, and turbulence *Phys. Rev. Lett.* **65** 3013
- [23] Veser G, Mertens F, Mikhailova S and Imbihl R 1993 Global coupling in the presence of defects: synchronization in an oscillatory surface reaction *Phys. Rev. Lett.* **71** 935
- [24] Rose K C, Battogtokh D, Mikhailov A, Imbihl R, Engel W and Bradshaw a M 1996 Cellular structures in catalytic reactions with global coupling *Phys. Rev. Lett.* **76** 3582
- [25] Rotermund H H 1999 Pattern formation in a surface reaction with global coupling *IMA Conf. on Pattern Formation in Continuous and Coupled Systems (Minneapolis)*
- [26] Ehsasi M, Frank O, Block J H and Christmann K 1990 Coupled chemical oscillators in catalytic oxidation of CO on Pd(110) surfaces *Chem. Phys. Lett.* **165** 115
- [27] Falcke M and Engel H 1994 Pattern formation during the CO oxidation on Pt(110) surfaces under global coupling *J. Chem. Phys.* **101** 6225
- [28] Graham M D, Kevrekidis I G, Asakura K, Lauterbach J, Krischer K, Rotermund H H and Ertl G 1994 Effects of boundaries on pattern formation: catalytic oxidation of CO on platinum *Science* **264** 80.
- [29] Graham M D, Bär M, Kevrekidis I G, Asakura K, Lauterbach J, Rotermund H H and Ertl G 1995 Catalysis on microstructured surfaces: pattern formation during CO oxidation in complex Pt domains *Phys. Rev. E* **52** 76